Evaluation of head injury criteria using a finite element model validated against experiments on localized brain motion, intracerebral acceleration, and intracranial pressure

doi:10.1533/ijcr.2005.0384

S Kleiven

CTV – Centre for Technology in Health Care, Royal Institute of Technology and Karolinska Institute, Stockholm, Sweden

Abstract: The objective of the present study was to analyze the effect of different load directions and durations following impact using a finite element (FE) model of the human head. A detailed FE model of the human head was developed and validated against available cadaver experiment data for three impact directions (frontal, occipital, and lateral). Loads corresponding to the same impact power were imposed in different directions. Furthermore, the head injury criterion (HIC), the recently proposed head impact power (HIP) criterion, as well as peak angular acceleration, and change in angular and translational velocity were evaluated with respect to the strain in the central nervous system (CNS) tissue. A significant correlation was found between experiments and simulations with regard to intracranial pressure data for a short-duration impulse and intracerebral acceleration characteristics for a long-duration impulse with a high-angular component. However, a poor correlation with the simulations was found for the intracranial pressures for the long-duration impulse. This is thought to be a result of air introduced to the intracranial cavity during experimental testing. Smaller relative motion between the brain and skull results from lateral impact than from a frontal or occipital blow for both the experiments and FE simulations. It was found that the influence of impact direction had a substantial effect on the intracranial response. When evaluating the global kinematic injury measures for the rotational pulses, the change in angular velocity corresponded best with the intracranial strains found in the FE model. For the translational impulse, on the other hand, the HIC and the HIP showed the best correlation with the strain levels found in the model.

Key words: Finite element method, head injury criterion, head impact power, impact direction, impact duration, brain displacement, intracranial pressure.

INTRODUCTION

Head injuries due to traffic accidents, at work and during leisure are major cause of death in Sweden and worldwide. Globally, the daily incidence rate of road accident injuries is estimated to 30 000 victims and 3000 deaths [1]. For people younger than 45 years the cost, estimated from years of life lost, resulting from road accidents is about six times higher than that from cancer [2]. In Sweden, the annual number of head injury cases is more than 20 000 [3]. The total annual rate of head injuries in Sweden over the last 14 years is relatively constant [3].

Thus, in spite of several national preventive strategies, there has not been any major impact on the total incidents of head injury cases. The main cause of death for people younger than 45 years of age in Sweden is either by road accidents or by poisoning [4]. When looking deeper into this cause of death for the younger part of the male population in Sweden, a clear pattern appears (Figure 1).

There has been increased interest for the use of finite element (FE) modeling for the human head during the last decade [5–13]. Perhaps, of greatest importance to FE modeling of the human head is the level to which a given model has been validated. Most models have been validated against the pressure data of Nahum et al. [14]. However, Bradshaw and Morfey [15] concluded that it is not acceptable to validate FE models for pressure and then use them for injury prediction. This is apparent since tissue level

Corresponding Author:
S Kleiven
CTV – Centre for Technology in Health Care
Royal Institute of Technology and Karolinska Institute, Stockholm, Sweden
Tel: +46-8-790 64 48 Fax: +46-8-21 83 68
Email: sveink@kth.se

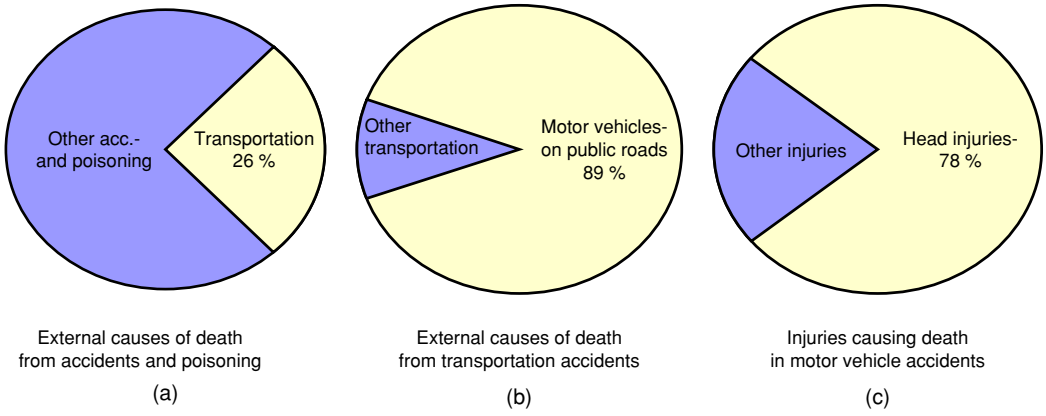

Figure 1 Head injuries are the main cause of traffic-related deaths in Sweden for males younger than 45 years of age. The results are derived from the main cause of death for this group of the population in 1999: accidents and poisoning.

models [16] have shown that diffuse axonal injury (DAI) is a function of strain and not pressure. The more relevant parameter for validation of an FE model of the human head should therefore be strain. Such data do not exist, but localized brain motion data are available, and provide a means of model validation that is more reliable.

Subdural hematomas (SDH) and diffuse axonal injuries are more lethal than most other brain lesions [17]. This is of special interest in deriving injury criteria for SDH and DAI. Gennarelli [18] suggested that SDH was produced by short duration and high amplitude of angular accelerations, while DAI was produced by longer duration and low amplitude of coronal accelerations. A threshold for DAI has been proposed [19], which accounts for rotational impulses in the coronal plane. The criterion is represented by curves of equal strain in an analytical model as a function of the angular acceleration and peak change of angular velocity. The curves show that for small changes in angular velocities, the injury is less dependent on the peak angular acceleration, while for high values of peak change in angular velocity, the injury is sensitive to the peak angular acceleration. This is in agreement with the hypothesis of Holbourn [20]. He stated that the shear strain, and thus injury, for long-duration impulses (large peak change in rotational velocity) is proportional to the acceleration, while the injury is proportional to the change of velocity for short-duration impacts.

Generally, the head injury criterion (HIC) [21] is used when evaluating the consequences of an impact to the head. HIC is based exclusively on the resultant, translational acceleration of the head. The basis underlying HIC was first introduced as a curve fit to the Wayne State Tolerance Curve (WSTC). The basic finding described by the WSTC was that high acceleration can be withstood for short durations, while lower accelerations can be tolerated for longer intervals.

Moreover, studies by Ueno and Melvin [22] and DiMasi et al. [23] found that the use of either translation or rotation alone may underestimate the severity of an injury. Recently, Zhang et al. [11] concluded that both linear and angular accelerations are significant causes of mild traumatic brain injuries. The generalized acceleration model for brain injury threshold (GAMBIT) was an early effort to combine thresholds for translational and rotational kinematics [24]. Because no dependency of the impulse duration is included, the GAMBIT can be seen as a peak-acceleration criterion for a combined rotational and translational impulse. Recently, a new global kinematic-based head injury criterion, called the head impact power (HIP), was presented [25]. In that study, it was proposed that coefficients for the different directions could be chosen to normalize the HIP with respect to some selected failure levels for a specific direction. However, values of the coefficients were not presented and information regarding directional sensitivity was lacking.

When a comparison between translation and rotation is performed, the usual approach has been to compare a non-centroidal rotational impulse with a translational impulse giving a similar acceleration measured at the center of gravity (c.g.) [5, 26]. This gives a good basis for study of head injury criteria based solely on the translational acceleration (i.e., HIC). In this case, however, the comparison will be between a translational impulse and an equal translational impulse in addition to the induced rotational one. A more objective approach could be to apply the same dosage of mechanical energy per time unit (the power) for the separate degrees of freedom as described here, and proposed as a new head injury criterion: HIP [25].

The influence of certain impact directions have been investigated for DAI [27, 28] and cerebral concussion [29]. In both studies, subhuman primates were used. In a three-dimensional (3D) numerical study [10], brain responses between frontal and lateral impacts were compared. This study confirmed earlier results by Gennarelli et al. [27] that loads in the lateral direction are more likely to cause DAI than impulses in the sagittal plane. Zhou et al. [6] suggested that SDH is more easily produced in an occipital impact than in a corresponding frontal one. Later, the same researchers [30] found that AP motion causes higher strain in the bridging veins than a corresponding lateral motion.

 doi:10.1533/ijcr.2005.0384

However, in all these numerical studies, a tied interface was imposed between the skull and the brain leaving out any possibility of evaluating relative motion induced injuries such as SDH. Recently, it was found that the influence of impact direction had a substantial effect in the prediction of subdural hematoma [31].

Thus, the aim of the present investigation was to study the influence of inertial forces on all the degrees of freedom of the human head, evaluated with a detailed FE model. Global injury measures such as magnitude in angular acceleration, change in angular and translational velocity, HIC, as well as HIP, were investigated with regard to their ability to take into account consequences of different impact directions and durations for the prediction of intracranial strains associated with injury.

Comprehensive correlation between FE model output and relative motion between the human cadaver brain and skull in anatomical X, Y, and Z components for different impact directions has only been demonstrated once previously [12]. Therefore, another goal of this study was to compare model results with cadaver experiments conducted for three impact directions: frontal, occipital (sagittal), and lateral (coronal).

METHODS

Finite element mesh

A detailed and parameterized FE model of the adult human head was created, comprising the scalp, skull, brain, meninges, cerebrospinal fluid (CSF), and 11 pairs of parasagittal bridging veins (Figure 2). A simplified neck, including an extension of the brain stem into the spinal cord, the dura and pia mater, and the vertebrae, was also modeled.

This model has been experimentally validated against pressure data in a previous study [32] as well as relative motion magnitude data [33]. Also, a comprehensive correlation between the FE model output and the relative motion between human cadaver brain and skull in anatomical X, Y, and Z components has been demonstrated for three impact directions [12]. The model has been validated with experiments performed using acceleration impulses of magnitudes and durations close to the ones in the present study.

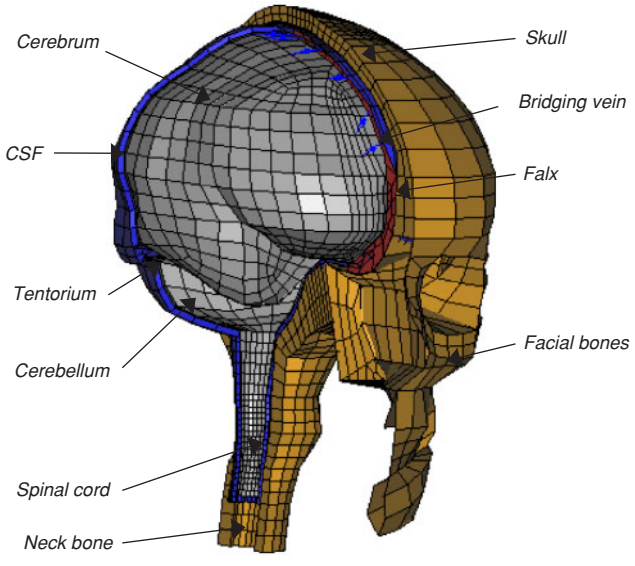

Figure 2 Finite element mesh of the human head.

Material properties

To cope with the large elastic deformations, a Mooney–Rivlin hyperelastic constitutive law was utilized for the central nervous system (CNS) tissues. Mendis et al. [34] derived the rate-dependent Mooney–Rivlin constants C_{10} and C_{01} and time decay constants β_i, using experiments published by Estes and McElhaney [35] on white matter from the corona radiata region.

According to Kleiven and Hardy [12], the average brain stiffness properties reported by Donnelly [36] showed the best correlation with experiments on localized motion of the brain. Previous studies [37, 38] have, on the other hand, indicated that the stiffness of the brain tissue might decrease after death. Therefore, Mooney–Rivlin constants corresponding to an effective (long-term) shear modulus of around 520 Pa was used for the analysis. The law was introduced for the white matter and the gray matter, which is reported to be insignificantly (about 4%) stiffer than the white matter [39]. The Mooney–Rivlin constants for the brain stem were assumed to be 80% higher than those for the gray matter in the cortex [40]. The stiffness parameters C_{10}, C_{01}, G_1, and G_2 were scaled while the decay constants were not altered. For the spinal cord and cerebellum, the same properties as for the white and gray matter were assumed due to lack of published data. A summary of the properties for the other tissues of the human head used in this study is shown in Table 1.

Interface conditions

The dura is often adhered to the skull, thus the interface between the skull and the dura was modeled with a tied contact definition in LS-DYNA [41]. Because of the presence of CSF between the meningeal membranes and the brain, sliding contact definitions were used for these interfaces. The chosen contact definition allowed sliding in the tangential direction and transfer of tension and compression in the radial direction. This was done in part because a fluid structure interface is likely to experience a vacuum when a pressure wave reflects at the contrecoup site, or when inertia forces create tension in brain regions opposite to the impact. An average CSF thickness of roughly 2 mm was used, which corresponds to approximately 120 ml of subdural and subarachnoidal CSF. A coefficient of friction of 0.2 was used, as proposed by Miller et al. [42].

 doi:10.1533/ijcr.2005.0384

Table 1 **Properties used in the numerical study**

Tissue	Young's modulus (MPa)	Density (kg/dm^3)	Poisson's ratio
Outer table/face	15 000	2.00	0.22
Inner table	15 000	2.00	0.22
Diploe	1000	1.30	0.24
Neck bone	1000	1.30	0.24
Brain	*Hyperelastic/viscoelastic*	1.04	~0.5
Cerebrospinal fluid	$K = 2.1$ GPa	1.00	0.5
Sinuses	$K = 2.1$ GPa	1.00	0.5
Dura mater	31.5	1.13	0.45
Falx/tentorium	31.5	1.13	0.45
Pia mater	11.5	1.13	0.45
Scalp	16.7	1.13	0.42
Bridging veins	EA = 1.9 N		

K, bulk modulus; EA, force/unit strain.

Experimental validation against localized brain motion data

Results from simulations with the FE model were compared with the relative displacement recordings from experiments presented by Hardy et al. [43], King et al. [44], and Kleiven and Hardy [12]. The cadaver head experiments focused on measuring the relative skull–brain motion using high-speed biplanar X-ray system and neutral density targets (NDT). The NDTs were implanted in two vertical columns located in the occipitoparietal region, and in the tempoparietal region, with a space between the centers of the NDTs of approximately 10 mm. The inverted cadaver head was suspended in a fixture that allowed rotation and translation. Frontal, occipital, and lateral impacts were conducted on the specimens. The rigid body motions of the skull were eliminated from the NDT (brain) motion data, leaving the skull–brain relative displacement data.

Experimental validation against intracranial pressure data for a short-duration impulse

Results from simulations with the FE model were compared with the intracranial pressure–time recordings from experiments conducted by Nahum et al. [14]. In order to reproduce the impact conditions, the anatomical plane of the model was inclined at about 45°, as in Nahum's experiments. In these experiments, cadaver heads were impacted to the frontal bone by a cylindrical load cell with a circular contact area. To increase the duration of the impact, Nahum et al. placed various paddings between the impactor and the scalp. The geometry and size of the impactor (6 inch cylindrical load cell), and the approximate thickness and type of padding material were measured and modeled. The padding on the impactor was modeled with a foam material model. The properties of the padding were adjusted so that the force versus time and acceleration characteristic of the experiment was largely reproduced. Model responses were compared with the measured cadaver test data in terms of impact force, head acceleration, and five epidural pressures: (1) frontal lobe and adjacent to the impact area, (2) immediately posterior and superior to the coronal and squamosal suture in the parietal area, (3) and (4) inferior to the lambdoidal suture in the occipital bone (one on each side of the sagittal plane), and (5) at the posterior fossa in the occipital area.

Experimental validation against intracranial pressure and intracerebral acceleration data for a long-duration impulse with a high-angular component

Results from simulations with the FE model were compared with the intracranial pressure–time and intracerebral acceleration–time recordings from experiments reported by Trosseille et al. [45]. For all tests, an accelerometer arrangement was screwed onto the skull in the occipital area in order to measure the head acceleration in three dimensions. Intracranial frontal, ventricular, and occipital pressures were also measured. The kinematics of this experiment was applied to the skull. The skull in this case was assumed to be a rigid body and six velocities were simulated. Model responses were compared with the measured cadaver test data in terms of three intracerebral accelerations: (1) frontal lobe, (2) lenticular nucleus, (3) occipital lobe, and five intracranial pressures: (1) frontal lobe, (2) occipital lobe, (3) temporal lobe, (4) third ventricle, and (5) lateral ventricle.

The results from the experiments and simulations were compared with regard to magnitudes and correlation coefficients.

Applied loads for study of directional influence

A total of nine acceleration pulses (pure translation and angular) were applied to the center of gravity of the head in the ±PA, ±SI, and in the lateral directions (Figure 3), in order to study directional differences. In the study of the angular acceleration components, a squared sinusoidal pulse ($\sin^2$) with an amplitude of 10–11.6 krad/s^2 and a duration of 5 ms, resulting in a peak angular velocity of 25–29 rad/s (in the range of the proposed threshold for

 doi:10.1533/ijcr.2005.0384

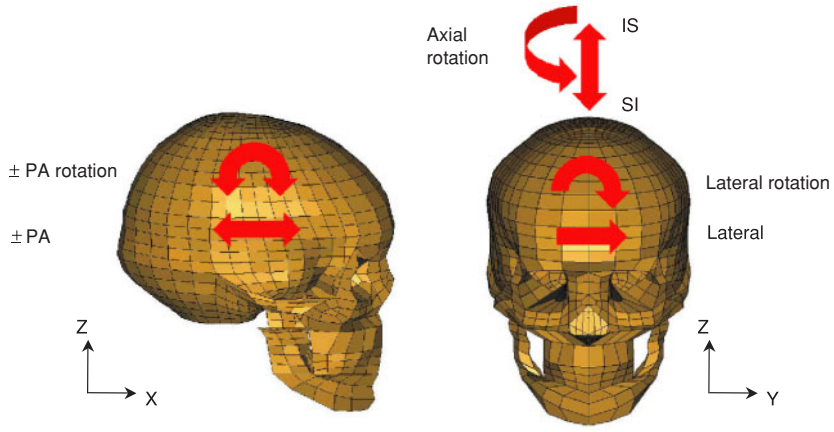

Figure 3 Load directions for translational and angular acceleration pulses.

DAI by Margulies and Thibault [19]), giving a HIP_{max} of 4.3 kW for all directions was used. To obtain a comparison with the angular impulses, a squared sinusoidal pulse with an amplitude of 794 m/s^2 (80 g) and a duration of 5 ms was used for the translational impulses, resulting in a HIC of 52 and a HIP_{max} of 4.3 kW.

Evaluation of HIP, α, and $\Delta\omega$ as an injury predictor for rotational kinematics

In addition to the directional study, the various global kinematic-based injury measures were evaluated using the same impulse shapes by keeping the measures constant and varying the impulse duration, as seen below. If the measure is correlating with strain (which is supposed to correlate with injury), applying a constant value of the injury measure (while varying the duration) would result in a constant strain in the model.

For the rotational kinematics, the peak angular acceleration, change in angular velocity, and HIP were evaluated. First, a constant AP angular acceleration impulse with an amplitude of 10 krad/s^2 was used. The duration was varied leading to a HIP_{max} of 1.08–17.3 kW and a change in angular velocity, $\Delta\omega$, of 6.25–50 rad/s. In addition, a constant change in angular velocity, $\Delta\omega$, of 25 rad/s was applied while the duration was varied leading to a HIP_{max} of 1.08–8.7 kW and a peak angular acceleration, α, of 2.5–20 krad/s^2. Finally, HIP was evaluated by keeping a constant value of 4.3 kW, while the duration was varied leading to a change in angular velocity, $\Delta\omega$, of 17.675–50 rad/s and a peak angular acceleration, α, of 5.0–14.14 krad/s^2.

Evaluation of HIC, HIP, and ΔV as an injury predictor for translational kinematics

For the translational AP direction, the HIC was evaluated by keeping a constant value of 1000 while the duration was varied leading to a change in velocity, ΔV, of 4.27–14.87 m/s and a peak acceleration of 1487–3417 m/s^2. In addition, the HIP and change in velocity were kept at a constant level of $HIP_{max} = 46$ kW and $\Delta V = 6.47$ m/s, respectively, for the various impulse durations.

The models were used to investigate the differences in terms of maximal principal strain in the brain due to variation in impact direction and duration. Furthermore, the HIC, the recently proposed HIP criterion, as well as peak angular acceleration and change in angular velocity were evaluated with respect to the strain in the CNS tissue. Thus, pulses of the same shape were applied to evaluate:

1. The sensitivity of impact direction by applying impulses resulting in constant values of HIP and HIC as previously described in Kleiven [31].
2. The proposed global kinematic-based injury measures (HIC, HIP, peak angular acceleration, and change in angular/translational velocity) by varying the duration and keeping the measure constant.

The maximal principal strain was chosen as a predictor of CNS injuries since it has been proposed as a predictor of diffuse axonal injuries [16].

RESULTS

Experimental validation against localized brain motion data

The results for the relative displacement of 12 locations in the occipitoparietal and temporoparietal regions for a 3 m/s frontal impact are shown in Figure 4. Each plot represents a given NDT location. The curves in the top half of the figure show relative displacement in the X direction, and the bottom curves show relative Z-direction displacement for the same locations. The motion of the markers is typically characterized by a maxima or minima occurring at around 25 ms before rebounding through the initial position (zero) at about 70 ms, and then reaching a minima or maxima at around 100 ms. There is a 0.7 mm (26.3%) average difference in X-displacement magnitudes between the experiment and simulation for the frontal impact. The smallest deviation in displacement magnitude (0.05 mm/2.1%) is found for marker NDTa5, while the largest difference (1.8 mm/48.5%) is found for NDTp6. The simulated Z-direction motion magnitudes deviate, in

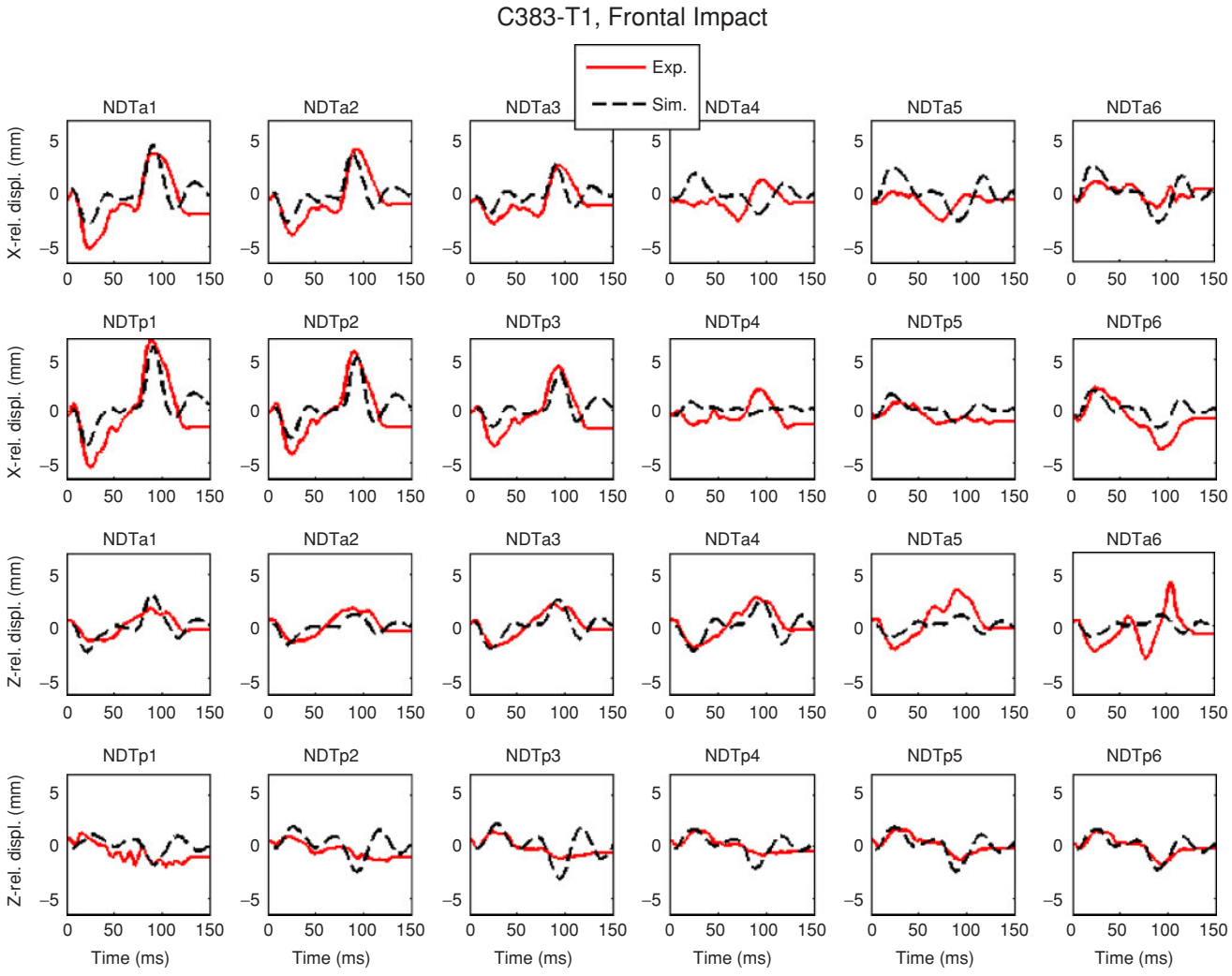

Figure 4 Simulation of relative motion in the sagittal plane for a frontal impact (C383-T1).

average, 1.0 mm (47.5%) from the experiments (ranging from 0.1 mm/5.9% for NDTa2 to 3.0 mm/72.5% for NDTa6). When it comes to the characteristics, an average correlation coefficient of 0.64 ($p < 0.001$) is found when comparing the experiments and simulations for the X-displacements for the whole time interval (0–150 ms). The lowest correlation coefficient is found for marker NDTa5 ($R = 0.35$, $p = 0.0017$), while the largest is found for NDTp1 ($R = 0.81$, $p < 0.0001$). The simulated Z-direction motion has, on average, a similar correlation in displacement characteristics as found for the X-direction having a correlation coefficient of 0.62 ($p < 0.001$) (ranging from $R = 0.32$, $p = 0.004$ for NDTa6 to $R = 0.84$, $p < 0.0001$ for NDTp6).

The results for the relative displacement of 10 locations in the occipitoparietal and temporoparietal regions for an occipital impact are shown in Figure 5. For the occipital impact (C755-T2) simulation, a better correlation between the model and the experimental results is seen when compared to the frontal impacts (Figure 5). There is a 0.4 mm/25.3% average difference in X-displacement magnitudes between the experiment and simulation for the occipital impact. The smallest deviation in displacement magnitude (0.07 mm/3.3%) is found for marker NDTp3, while the largest difference (1.7 mm/107.8%) is found for NDTa5. The simulated Z-direction motion magnitudes deviate, in average, 0.6 mm/31.9% from the experiments (ranging from 0.04 mm/1.3% for NDTp3 to 1.3 mm/91.7% for NDTa2). When it comes to the characteristics, an average correlation coefficient of 0.82 ($p = 0.0025$) is found when comparing the experiments and simulations for the X-displacements for the whole time interval (0–150 ms). The lowest correlation coefficient is found for marker NDTp4 ($R = 0.40$, $p = 0.024$), while the largest is found for NDTa2 ($R = 0.97$, $p < 0.0001$). The simulated Z-direction motion characteristic has, on average, a correlation coefficient of 0.73, $p = 0.009$ (ranging from $R = 0.31$, $p = 0.087$ for NDTa1 to $R = 0.97$, $p < 0.0001$ for NDTp5).

When simulating the lateral impact, characteristics similar to those seen in the experiment were found for Y and Z displacements (Figure 6). The motion of the brain

 doi:10.1533/ijcr.2005.0384

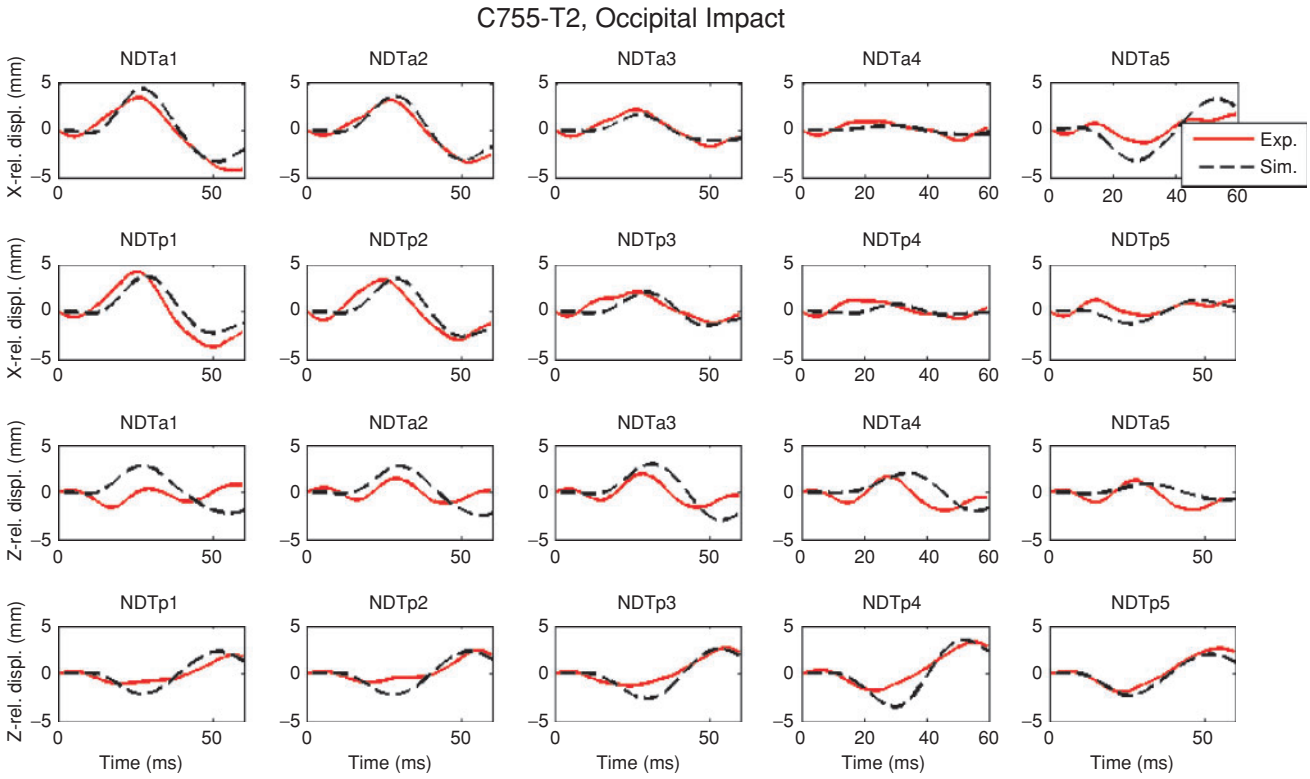

Figure 5 Simulation of relative motion in the sagittal plane for an occipital impact (C755-T2).

targets relative to the skull shows a characteristic peak around 10–15 ms, which subsequently decays. When comparing the experimental Y-displacement magnitudes to the simulation at this initial peak, a 0.7 mm/38.5% average difference was found. The smallest deviation in Y-displacement magnitude (0.02 mm/0.6%) is found for marker NDTaL2, while the largest difference (2.0 mm/49.5%) is found for NDTaL4. The simulated Z-direction motion magnitudes deviate, in average, 0.8 mm/62.1% from the experiments (ranging from 0.1 mm/9.9% for NDTaL1 to 2.1 mm/173.9% for NDTaL3). When it comes to the characteristics, an average correlation coefficient of 0.68 ($p = 0.002$) is found when comparing the experiments and simulations for the Y-displacements for the whole time interval (0–100 ms). The lowest correlation coefficient is found for marker NDTpL3 ($R = 0.33$, $p = 0.016$), while the largest is found for NDTaL5 ($R = 0.95$, $p < 0.0001$). The simulated Z-direction motion characteristic has, on average, a correlation coefficient of 0.43, $p = 0.12$ (ranging from $R = 0.03$, $p = 0.85$ for NDTpL2 to $R = 0.76$, $p < 0.0001$ for NDTaL5).

Experimental validation against intracranial pressure data for a short-duration impulse

The predicted intracranial pressure responses from the FE model agreed well with previously published recordings during a short-duration frontal impact [14]. As seen from Figures 7 and 8, the calculated curves for the impactor force, head acceleration, and pressures gave magnitudes and characteristics similar to the experimental results. The sliding interface without separation provided a way to allow sliding while giving tensile resistance in countercoup areas. There is a 32 N (0.4%) difference in the maximal force between the experiment and simulation for the frontal impact. When comparing the experimental acceleration magnitude to the simulation, a difference of 51 m/s^2 (2.5%) was found. The simulated impact force characteristic has a correlation coefficient of 0.97 ($p < 0.0001$) to the experimental one, while a correlation coefficient of 0.78 ($p < 0.0001$) is found for the acceleration. Looking at the frontal pressure, there is a 3.5 kPa (2.5%) difference between the experiment and simulation, while the occipital #1, occipital #2, temporal, and posterior fossae pressures have differences of 1.7 kPa (3.8%), 4.7 kPa (9.7%), 0.2 kPa (0.3%), and 0.4 kPa (0.7%), respectively. The simulated frontal pressure characteristic has a correlation coefficient of 0.98 ($p < 0.0001$) to the experimental one, while correlation coefficients of 0.89 ($p < 0.0001$) and 0.52 ($p = 0.045$) are found for the occipital #1 and #2 pressures, respectively. For the temporal and posterior fossae pressures, correlation coefficients of 0.97 ($p < 0.0001$) and 0.75 ($p = 0.0013$) are found.

Experimental validation against intracranial pressure and intracerebral acceleration data for a long-duration impulse with a high-angular component

Simulation results from Figure 9 show that a realistic simulation of the intracerebral acceleration is possible for

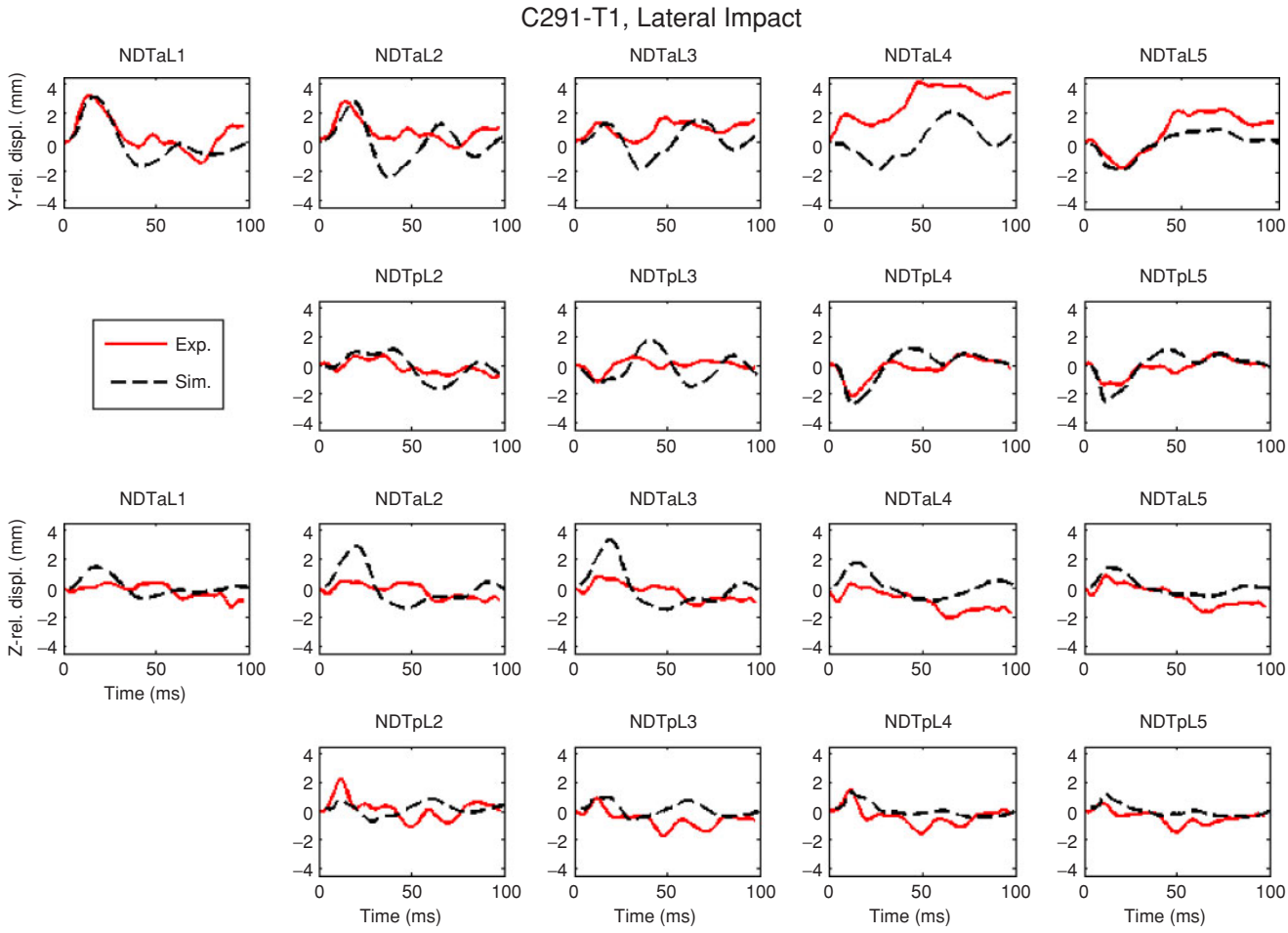

Figure 6 Simulation of relative motion in the coronal plane for a lateral impact (C291-T1).

long-duration impacts with a high-angular component. However, for this particular experiment, it was found that the correlations with simulations for the intracranial pressures are quite poor for most locations (Figure 10). When comparing the experimental intracerebral acceleration magnitudes to the simulations, a difference of 0.9 m/s^2 (1.3%) was found for the frontal lobe, while differences of 11.1 m/s^2 (15.0%) and 0.4 m/s^2 (0.6%) were found for the lenticular nucleus and occipital lobe, respectively. The simulated intracerebral acceleration characteristics have correlation coefficients ranging from 0.85 for the frontal lobe to 0.94 for the occipital lobe to the experimental ones ($p < 0.0001$). Looking at the frontal pressure, there is a 34 kPa (38.7%) difference between the experiment and simulation, while the occipital, temporal, third ventricle, and lateral ventricle pressures have differences of 22.8 kPa (183.5%), 3.3 kPa (32.3%), 17.1 kPa (40.0%), and 18.5 kPa (41.9%), respectively. The simulated frontal pressure characteristic has a correlation coefficient of 0.09 ($p = 0.19$) to the experimental one, while correlation coefficients of 0.73 ($p < 0.001$) and 0.26 ($p < 0.001$) are found for the occipital and temporal pressures, respectively. For the third and lateral ventricle pressures, correlation coefficients of 0.13 ($p = 0.058$) and 0.04 ($p = 0.62$) are found.

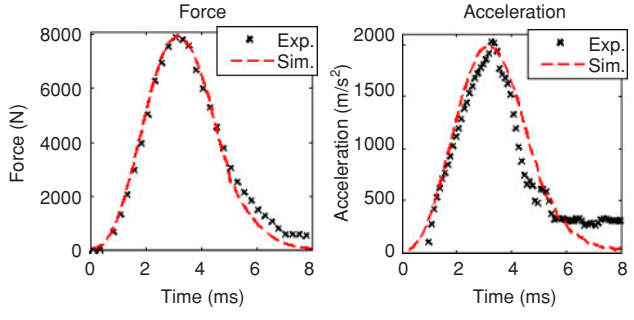

Figure 7 Force and acceleration response from simulation of the cadaver experiments by Nahum et al. [14] when impacting the head model using a 6 inch, padded impactor having an initial velocity of 9.94 m/s and a mass of 5.59 kg.

Directional sensitivity

A summary of the results from the comparison of translational and angular impulses in different directions is shown in Figure 11. It can be seen that the largest strain on the brain appears for the lateral and axial rotational impulses, while substantially smaller strain is found for the translational impulses (Figure 11).

 doi:10.1533/ijcr.2005.0384

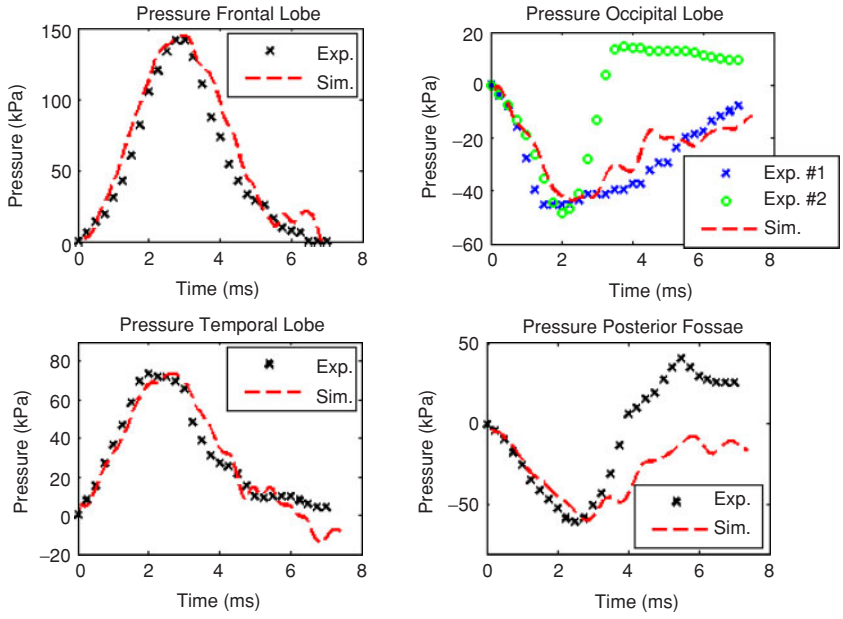

Figure 8 Simulation of the pressure results from the cadaver experiments by Nahum et al. [14] by impacting the head model using a 6 inch, padded impactor having an initial velocity of 9.94 m/s and a mass of 5.59 kg.

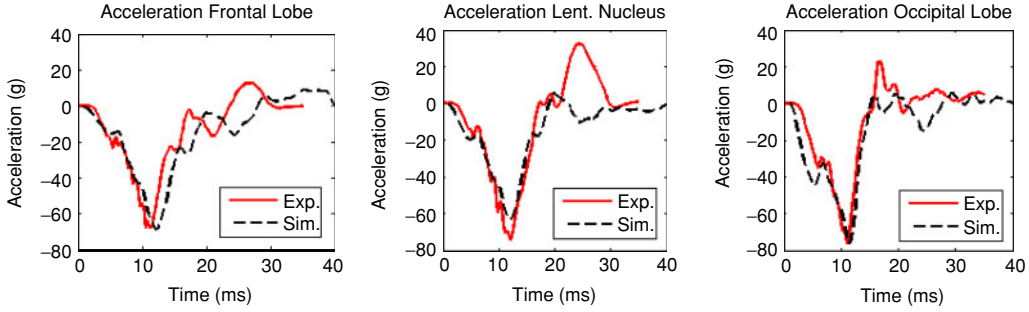

Figure 9 Simulation of the intracerebral acceleration results from the cadaver experiments by Trosseille et al. [45].

For the angular impulses, the same HIP_{max} values are calculated as for the translational impulses, while the HIC is equal to zero for a pure rotational impulse. Nevertheless, larger strains on the brain appear for the rotational impulses. For this type of loading, the worst case is the lateral rotation where the highest strain on the cortex, corpus callosum, and brain stem appears. Almost a 10-fold increase in the intracranial strains is found for the PA and AP impulses, when switching from a translational to a rotational mode of motion.

Images showing a parasagittal view of the straining of the brain when enduring the AP rotational and AP translational impulses simulating a frontal impact can be seen in Figure 12. Note the high levels of strain close to the vertex of the skull as well as close to the irregularities in skull base for the rotational impulse. Correspondingly, low levels of strain can be seen in the vicinity of the ventricles. A pure AP rotation is not likely to occur in real life, but can be very closely compared with an uppercut in boxing, while large AP translational accelerations can be experienced during a frontal collision.

Figure 13 shows the strain distribution in a mid-coronal cross-section for the lateral rotational impulse (Figure 13, upper left) and a sagittal view of a inferior–superior (IS) translational motion (Figure 13, lower right). Note the high levels of strain in the corpus callosum area, and close to the brain stem for the lateral rotation. For the IS impulse, the highest strains can be noted in the spinal cord as well as around and close to the brain stem and cerebellum. An impulse with a high level of lateral rotation could occur in a side impact during an automotive or pedestrian accident, while a pure IS translational motion can be compared with a fall accident or a helicopter crash-landing.

Evaluation of HIP, α, and $\Delta\omega$ as an injury predictor for rotational kinematics

When evaluating the various global kinematic-based injury measures for an AP rotational motion by keeping the various measures constant while varying the impulse duration, it was found that the change in angular velocity mirrored the level of strain on the brain better than the HIP and the peak angular acceleration did. An almost constant level of

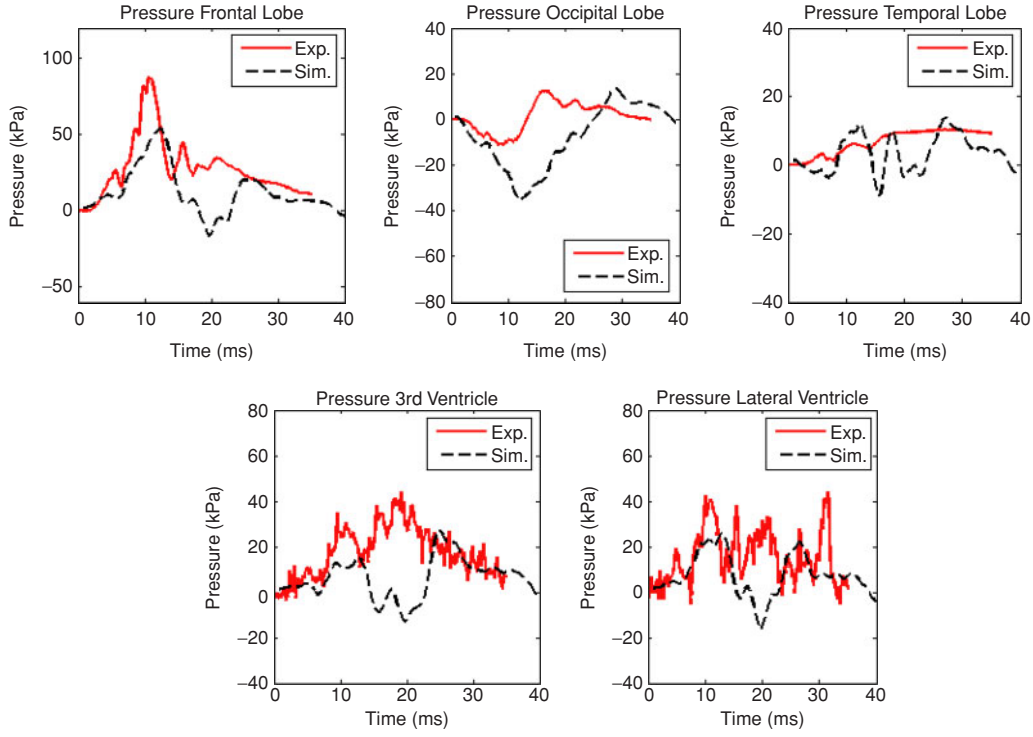

Figure 10 Simulation of the intracranial pressure results from the cadaver experiments by Trosseille et al. [45].

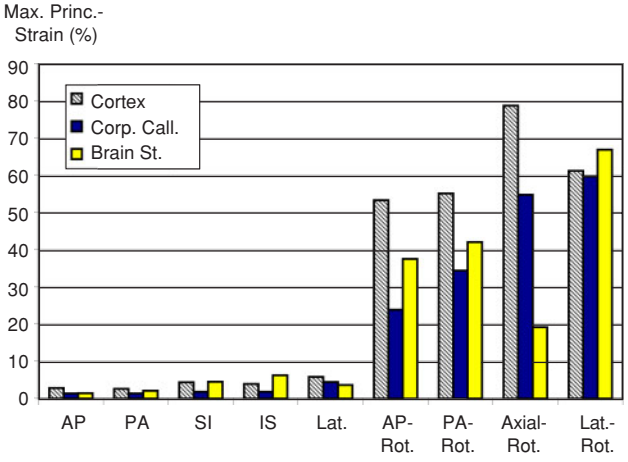

Figure 11 Results for different directions and translational and angular acceleration impulses. $HIP_{max} = 4.3$ kW, HIC = 0 for the angular impulses, while $HIP_{max} = 4.3$ kW and HIC = 52 for the translational impulses.

strain was found for a constant change in angular velocity, while both the HIP and the peak angular acceleration gave an increasing strain level for an increase in the impulse duration (Figure 14).

Evaluation of HIC, HIP, and ΔV as an injury predictor for translational kinematics

When evaluating the various global kinematic-based injury measures for an AP translational motion by keeping the various measures constant while varying the impulse duration, it was found that the HIC and HIP mirrored the level of strain in the brain better than the change in velocity did. An almost constant level of strain was found for a constant HIC and HIP, while a constant change in velocity gave a decreasing strain level for an increase in impulse duration (Figure 15).

DISCUSSION

The present results verify the hypothesis that a variation in load direction alters the outcome of an impact to the human head. Based on this FE model, new global head injury criteria can be evaluated for all the degrees of freedom of the head. Hence, the injury criteria are valid for a larger span of impact conditions. Injury criteria are at present based on a few load directions, but in real life and as indicated by this study, the worst cases for different intracranial components vary depending on the load direction.

The findings of larger stresses and strains in the corpus callosum for the lateral angular acceleration impulse as well as the lateral translational impulse support the conclusions drawn by Gennarelli et al. [27, 28] that loads in the lateral direction are more likely to cause DAI compared to impulses in the sagittal plane. The largest strains, on the other hand, occurred on the surface of the cortex area. However, large stresses and strains on the surface of the cortex area are related to cortical contusions, and such injuries are usually less critical than the devastating DAI associated with shear strains and effective stresses in the corpus callosum and brain stem areas [46]. Strich [47] found

 doi:10.1533/ijcr.2005.0384

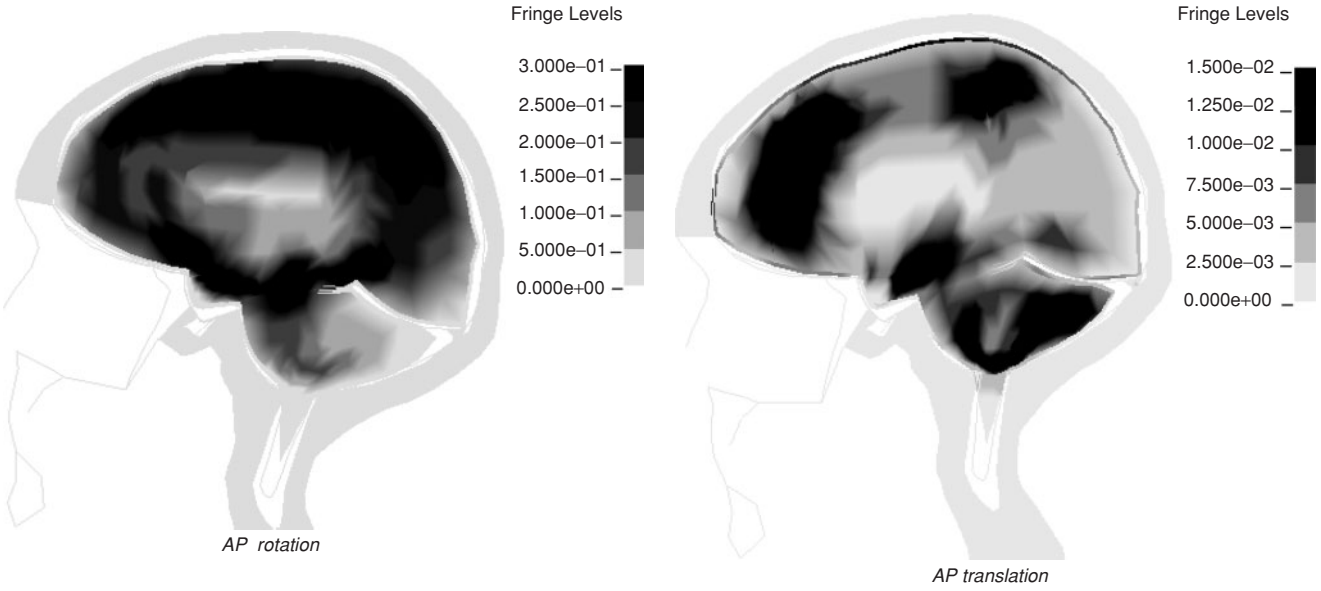

Figure 12 Strain distribution (around maximum) for AP rotation (left) and AP translation (right) using the same duration, impulse shape, giving the same HIP, and resulting in substantially different intracranial strains.

diffuse degeneration of white matter in the cerebral hemispheres, as well as in the brain stem and corpus callosum areas in patients who have endured severe head trauma. This indicates that high-shear strain in the white matter adjacent to the cortex is likely to occur in a real life accident. Correspondingly, low levels of strain can be seen in the vicinity of the ventricles in the model, which supports the hypothesis that a strain relief is present around the ventricles [48].

A zero HIC value is predicted for a pure rotational impulse, while higher levels of stresses and strains are found compared to a corresponding translational impulse in the same direction. This underlines findings by previous investigators [49]. Gennarelli et al. [49] subjected 25 squirrel monkeys to controlled sagittal plane head motions, and found brain lesions in both translated and rotated groups, but with greater frequency and severity after rotation. This is consistent with the results presented herein, as well as the hypothesis presented by Holbourn [20]. Regarding the translational impulses, larger strains occurred in the spinal cord and brain stem area for the axial impulses (IS and SI) compared to the sagittal AP and PA impulses. For the SI and the IS translational impulses, the upper part of the spinal cord, and thus the lower part of the brain stem, is likely to endure large inertia forces when accelerated in the axial direction. This stretching of the brain stem has previously been discussed in Hodgson and Thomas [50], who suggested that the mechanism of brain stem injury, regardless of head motion, is due to shear caused by stretching of the cervical cord. Axial accelerations are usually caused by accidents due to fall and clinical observations show that this may lead to DAI in the brain stem as well as tearing injuries to the posterior fossa tentorium [51]. The findings of high strain in the central parts of the brain and lower strains in the brain stem for the axial rotational impulse support the findings of Gennarelli et al. [28] that horizontal impulses almost exclusively produce DAI in the central parts of the brain.

An almost constant level of strain was found for a constant change in angular velocity, while both the HIP and the peak angular acceleration gave an increasing strain level for an increase in the impulse duration for the AP rotational motion (Figure 14). This corresponds to Holbourn's hypothesis [20] that the strain (and the injury) is proportional to the change in angular velocity for rotational impulses of short durations. For the corresponding translational motion, on the other hand, an almost constant level of strain was found for a constant HIC and HIP, while for a constant change in velocity a decreasing strain level for an increase in the impulse duration occurred (Figure 15). This supports the results presented by Newman et al. [25], where a good correlation was found between concussion and both the HIC and the HIP for predominantly translational impact data. Because most of the previously proposed angular thresholds are based on non-centroidal rotation in primate experiments, followed by analytical scaling techniques, the applicability of thresholds for humans might be discussed. Also, studies on volunteer boxers [52] suggest that the human tolerance is largely underestimated while using primates for experiments and simplistic scaling rules.

The local motion of brain tissue described by Hardy et al. [43], King et al. [44], and Kleiven and Hardy [12] has been simulated for three impact directions (frontal, occipital, and lateral). Both the model and the experiments show similar magnitudes of relative motion between the skull and the brain for the occipital and frontal impact scenarios. The lateral impact resulted in smaller relative motion than the frontal impact of similar severity. This is true

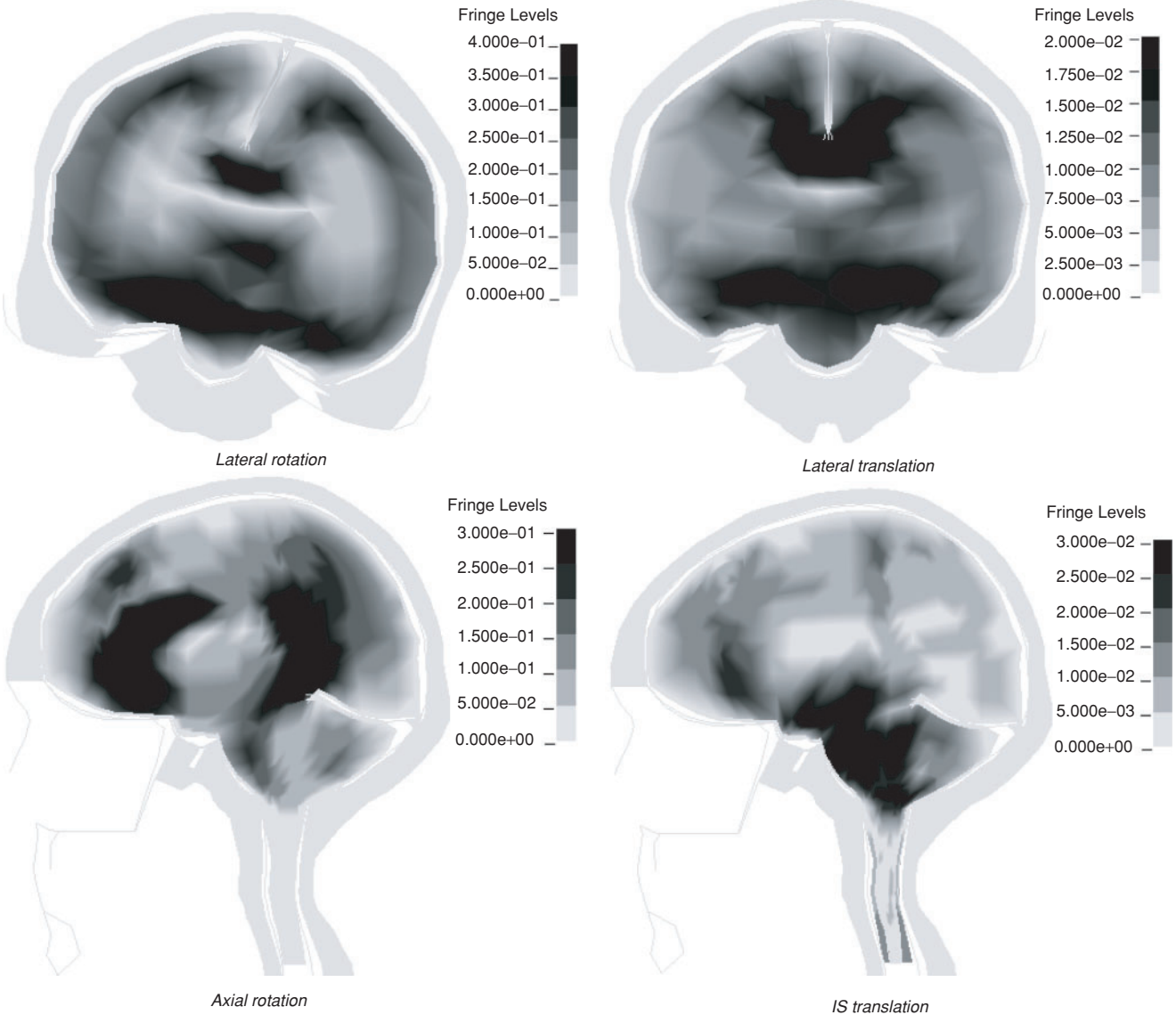

Figure 13 Strain distribution (around maximum) for lateral rotation (upper left), lateral translation (upper right), axial rotation (lower left), and IS translation (lower right) using the same duration and impulse shape, resulting in the same HIP.

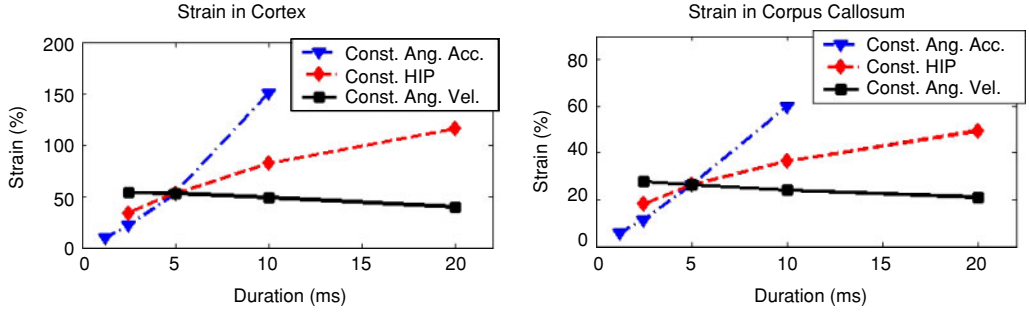

Figure 14 Evaluation of global kinematic measures for rotational motion; keeping the magnitudes of angular acceleration, change in angular velocity, and the HIP, respectively, constant while varying the impulse duration.

 doi:10.1533/ijcr.2005.0384

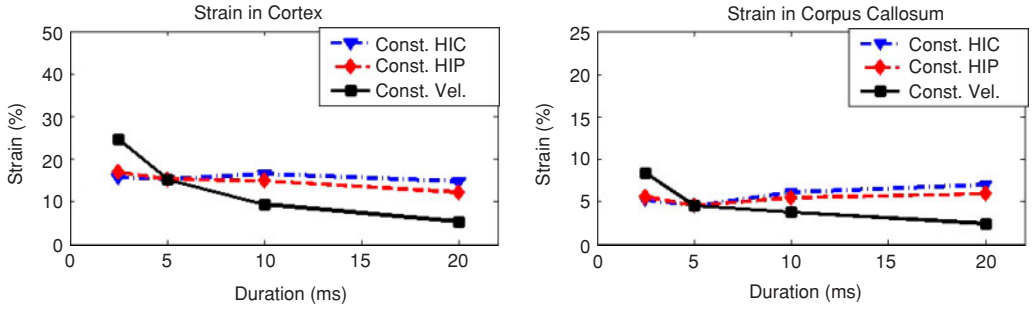

Figure 15 Evaluation of global kinematic measures for translational motion; keeping the magnitudes of HIC, HIP, and change in velocity, respectively, constant while varying the impulse duration.

for the cadaver experiments and the simulations. This is mainly thought to be due to the supporting structure of the falx cerebri. Gennarelli et al. [27, 28] produced traumatic coma in monkeys by accelerating the head without impact in various non-centroidal rotation scenarios. It was found that the majority of the animals that were subjected to coronal rotation suffered more prolonged coma. Also, all the laterally impacted animals had a degree of DAI in the corpus callosum and superior cerebellar peduncle similar to that found in severe human head injury. The present study supports the findings of Gennarelli et al. [27, 28]: smaller relative motion between the brain and skull suggests the influence of the falx, which may impinge upon adjacent structures such as the corpus callosum, potentially causing injury. This is also supported by the findings of higher strains in the corpus callosum for coronal rotation compared to sagittal rotation when imposing a sinusoidal acceleration pulse corresponding to the same head impact power.

Comparison of results from the FE model with experimental measurements of intracranial pressures presented by Nahum et al. [14] shows a good correlation reaching the magnitudes of the relative displacements in the experiments. The exact timing of the acceleration impulse relative to the impact for the Nahum experiment is not known. This makes it difficult to compare any temporal differences. There are obvious differences between the experimental pressure data and the simulations, especially in the occipital region. However, since the differences between the right and left pressures (occipital #1 and occipital #2) reported in Nahum et al. [14] are greater than the differences between experiments and simulations, the differences between the experiments and simulations can be considered to be small. A further difficulty experienced by Nahum et al. [14], when conducting the experiments, was the presence of motion in the lateral direction. To minimize this out-of-plane motion, sutures were attached to the ears of the test subjects prior to impact. This (although minimized) lateral motion, as well as the influence of the sutures, would probably also affect the results, and are not accounted for in the simulations.

The lack of symmetry in the magnitudes of the frontal and occipital pressures seen in the experiments by Trosseille et al. is likely to be due to the presence of air in the intracranial cavity. This lack of symmetry can be seen in both the MS428 experiments as well as for MS408. It was proposed in Trosseille et al. [45] that a possible reason for this was the presence of air in the cerebrospinal fluid. This would also explain the correlation between simulation and experiment in intracerebral accelerations, measured inside the brain tissue, while the intracranial pressures taken from similar locations, but at the skull brain surface, do not correlate so well.

In summary, regarding the influence of inertial forces to all the degrees of freedom of the human head, this study shows:

1. HIC is unable to predict consequences of a pure rotational impulse while HIP and peak change in velocity needs individual scaling coefficients for the different terms to account for a difference in load direction.
2. For a purely rotational impulse, the peak change in angular velocity shows the best correlation with the strain levels found in the FE model.
3. For a purely translational impulse, the HIC and the HIP show the best correlation with the strain levels found in the FE model.

ACKNOWLEDGMENTS

The author would like to thank Professor Hans von Holst of the Royal Institute of Technology, Stockholm, for his helpful suggestions and valuable assistance. The author also wishes to thank Ted Bloomquist, San Diego, USA, for providing reliable input data for the intracranial pressure experiment published by Nahum et al. [14]. Appreciation is extended to Warren N. Hardy of the Wayne State University Bioengineering Center, Detroit, USA for giving me an opportunity to assist in parts of the localized motion experiments used in the present study and previously published by Hardy et al. [43].

REFERENCES

1. C J L Murray and A D Lopez, *The Global Burden of Disease Summary*, Cambridge, MA, Harvard University Press, 1996

2. European Transport Safety Council, 'Reducing the severity of road injuries through post impact care', ISBN: 90-76024-07-3, 1999.
3. S Kleiven, P M Peloso and H von Holst, 'The epidemiology of head injuries in Sweden from 1987 to 2000', *J Inj Control Saf Promot*, 2003 **10** (1) 173–180.
4. National Board of Health and Welfare, Centre for Epidemiology, http://www.sos.se/epc/epceng.htm, Stockholm, Sweden, 2001.
5. F A Bandak and R H Eppinger, 'A three-dimensional FE analysis of the human brain under combined rotational and translational accelerations', Proc 38th stapp car crash conf, Society of Automotive Engineers, Warrendale, PA, 1994, pp. 145–163.
6. C Zhou, T B Khalil and A I King, 'A new model comparing impact responses of the homogeneous and inhomogeneous human brain', Proc 39th stapp car crash conf, SAE Technical Paper No. 952714, Society of Automotive Engineers, Warrendale, PA, 1995, pp. 121–137.
7. R Willinger, L Taled and P Pradore, 'Head biomechanics: from the finite element model to the physical model', Proc IRCOBI conf, Brunnen, Switzerland, International Research Council on the Biomechanics of Impact, Bron, France, 1995, pp. 245–260.
8. J S Ruan, T B Khalil and A I King, 'Impact head injury analysis using an explicit finite element human head model', *J Traffic Med*, 1997 **25** 33–40.
9. M Claessens, F Sauren and J Wismans, 'Modeling of the human head under impact conditions: a parametric study', Proc 41st stapp car crash conf, SAE Paper No. 973338, Society of Automotive Engineers, Warrendale, PA, 1997, pp. 315–328.
10. L Zhang, K H Yang and A I King, 'Comparison of brain responses between frontal and lateral impacts by finite element modeling', *J Neurotrauma*, 2001 **18** (1) 21–30.
11. L Zhang, K H Yang and A I King, 'A proposed injury threshold for mild traumatic brain injury', *J Biomech Eng*, 2004 **126** (1) 226–236.
12. S Kleiven and W N Hardy, 'Correlation of an FE model of the human head with experiments on localized motion of the brain – consequences for injury prediction', 45th stapp car crash journal, SAE Paper No. 02S-76, Society of Automotive Engineers, Warrendale, PA, 2002.
13. T J Horgan and M D Gilchrist, 'The creation of three-dimensional finite element models for simulating head impact biomechanics', *Int J Crashworthiness*, 2003 **8** (3) 1–14.
14. A M Nahum, R Smith and C Ward, 'Intracranial pressure dynamics during head impact', Proc 21st stapp car crash conf, SAE Paper No. 770922, Society of Automotive Engineers, Warrendale, PA, 1977, pp. 337–366.
15. D R S Bradshaw and C L Morfey, 'Pressure and shear response in brain injury models', Proc 17th int tech conf *Enhanced Safety of Vehicles*, Amsterdam, The Netherlands, 2001.
16. B C Bain and D F Meaney, 'Tissue-level thresholds for axonal damage in an experimental model of central nervous system white matter injury', *J Biomech Eng*, 2000 **16** 615–622.
17. T A Gennarelli and L E Thibault, 'Biomechanics of acute subdural hematoma', *J Trauma*, 1982 **22** (8) 680–686.
18. T A Gennarelli, 'Head injuries in man and experimental animals: clinical aspects', *Acta Neurochir Suppl*, 1983 **32** 1–13.
19. S S Margulies and L E Thibault, 'A proposed tolerance criterion for diffuse axonal injury in man', *J Biomech*, 1992 **25** (8) 917–923.
20. A H S Holbourn, 'Mechanics of head injury', *Lancet*, 1943 **2** (October 9) 438–441.
21. National Highway Traffic Safety Administration, Department of Transportation (DOT), 'Occupant crash protection – head injury criterion S6.2 of MVSS 571.208', Docket 69-7, Notice 17, NHTSA, Washington, DC, 1972.
22. K Ueno and J W Melvin, 'Finite element model study of head impact based on hybrid III head acceleration: the effects of rotational and translational acceleration', *J Biomech Eng*, 1995 **117** (3) 319–328.
23. F DiMasi, R H Eppinger and F A Bandak, 'Computational analysis of head impact response under car crash loadings', Proc 39th stapp car crash conf, SAE Paper No. 952718, Society of Automotive Engineers, Warrendale, PA, 1995, pp. 425–438.
24. J A Newman, 'A generalized acceleration model for brain injury threshold', Proc IRCOBI conf, 1986, pp. 121–131.
25. J A Newman, N Shewchenko and E Welbourne, 'A proposed new biomechanical head injury assessment function – the maximum power index', Proc 44th stapp car crash conf, SAE Paper No. 2000-01-SC16, 2000.
26. S S Margulies, L E Thibault and T A Gennarelli, 'A study of scaling and head injury criteria using physical model experiments', Proc 1985 int IRCOBI/AAAM conf *Biomechanics of Impacts*, Göteborg, Sweden, 1985, pp. 223–235.
27. T A Gennarelli, L E Thibault, J H Adams, et al., 'Diffuse axonal injury and traumatic coma in the primate', *Ann Neurol*, 1982 **12** 564–574.
28. T A Gennarelli, L E Thibault, G Tomei, et al., 'Directional dependence of axonal brain injury due to centroidal and non-centroidal acceleration', Proc 31st stapp car crash conf, SAE Paper No. 872197, Society of Automotive Engineers, Warrendale, PA, 1987, pp. 49–53.
29. V R Hodgson, L M Thomas and T B Khalil, 'The role of impact location in reversible cerebral concussion', Proc 27th stapp car crash conf, SAE Paper No. 831618, Society of Automotive Engineers, Warrendale, PA, 1983, pp. 225–240.
30. C Zhou, T B Khalil and A I King, 'Visoelastic response of the human brain to sagittal and lateral rotational acceleration by finite element analysis', Proc 1996 IRCOBI conf, Dublin, Ireland, Technical Paper No. 1996-13-0003, 1996.
31. S Kleiven, 'Influence of impact direction to the human head in prediction of subdural hematoma', *J Neurotrauma*, 2003 **20** (4) 365–379.
32. S Kleiven and H von Holst, 'Consequences of head size following trauma to the human head', *J Biomech*, 2002a **35** (2) 153–160.
33. S Kleiven and H von Holst, 'Consequences of brain volume following impact in prediction of subdural hematoma evaluated with numerical techniques', *Traffic Inj Prevent*, 2002b **3** (4) 303–310.
34. K K Mendis, R L Stalnaker and S H Advani, 'A constitutive relationship for large deformation finite element modeling of brain tissue', *J Biomech Eng*, 1995 **117** (4) 279–285.
35. M S Estes and J H McElhaney, 'Response of brain tissue to compressive loading', ASME Paper No. 70-BHF-13, 1970.
36. B R Donnelly, 'Brain tissue material properties: a comparison of results. Biomechanical research: experimental and computational', Proc 26th int workshop, 1998, pp. 47–57.
37. H Metz, J McElhaney and A K Ommaya, 'A comparison of the elasticity of live, dead, and fixed brain tissue', *J Biomech*, 1970 **3** 453–458.

 doi:10.1533/ijcr.2005.0384

38. R L Stalnaker, J W Melvin, G S Nusholtz, N M Alem and J B Benson, 'Head impact response', Proc 42nd stapp car crash conf, SAE Paper No. 770921, Society of Automotive Engineers, Warrendale, PA, 1977.
39. M T Prange, D F Meaney and S S Margulies, 'Defining brain mechanical properties: effects of region, direction, and species', Proc 44th stapp car crash journal, SAE Paper No. 2000-01-SC15. The Stapp Association, Ann Arbor, MI, 2000.
40. K B Arbogast and S S Margulies, 'Regional differences in mechanical properties of the porcine central nervous system', Proc 41st stapp car crash conf, SAE Paper No. 973336, Society of Automotive Engineers, Warrendale, PA, 1997, pp. 293–300.
41. Livermore Software Technology Corporation, *LS-DYNA Keyword User's Manual*, Version 960, 2001.
42. R T Miller, S S Margulies, M Leoni, et al., 'Finite element modeling approaches for predicting injury in an experimental model of severe diffuse axonal injury', Proc 42nd stapp car crash conf, SAE Paper No. 983154, Society of Automotive Engineers, Warrendale, PA, 1998, pp. 155–166.
43. W N Hardy, C Foster, M Mason, K Yang, A King and S Tashman, 'Investigation of head injury mechanisms using neutral density technology and high-speed biplanar X-ray', 45th stapp car crash journal, The Stapp Association, Ann Arbor, MI, 2001, pp. 337–368.
44. A I King, W N Hardy, M J Mason and S Tashman, 'Comparison of relative motion between the brain and skull of the human cadaver for rotation in the coronal and sagittal planes', 4th world congr *Biomechanics*, Calgary, Alberta, Canada, August 2002.
45. X Trosseille, C Tarrière, F Lavaste, F Guillon and A Domont, 'Development of a FEM of the human head according to a specific test protocol', Proc 36th stapp car crash conf, SAE Paper No. 922527, Society of Automotive Engineers, Warrendale, PA, 1992, pp. 235–253.
46. J W Melvin, J W Lighthall and K Ueno, 'Brain injury biomechanics', *Accidental Injury*, A M Nahum and J W Melvin (Eds.), Springer-Verlag, New York, 1993, pp. 269–290.
47. S J Strich, 'Diffuse degeneration of the cerebral white matter in severe dementia following head injury', *J Neurol Neurosurg Psychiatr*, 1956 **19** (October 9) 163–185.
48. J Ivarsson, D C Viano, P Lövsund and B Aldman, 'Strain relief from the cerebral ventricles during head impact: experimental studies on natural protection of the brain', *J Biomech*, 2000 **33** (2) 181–189.
49. T A Gennarelli, L E Thibault and A K Ommaya, 'Pathophysiological responses to rotational and translational accelerations of the head', Proc stapp car crash conf, SAE Paper No. 720970, Society of Automotive Engineers, Warrendale, PA, 1972, pp. 296–308.
50. V R Hodgson and L M Thomas, 'Acceleration induced shear strains in a monkey brain hemisection', 23rd stapp car crash conf, SAE Paper No. 791023, Society of Automotive Engineers, Warrendale, PA, 1979.
51. R Dirnhofer, F Walz and T Sigrist, 'Zur mechanischen belastbarkeit des tentorium cerebelli', *Z Rechtsmed*, 1979 **82** 305–311.
52. Y Pincemaille, X Trosseille, P Mack, C Tarrière, F Breton and B Renault, 'Some new data related to human tolerance obtained from volunteer boxers', 33rd stapp car crash conf, SAE Paper No. 892435, Society of Automotive Engineers, Warrendale, PA, 1989, pp. 177–190.

 doi:10.1533/ijcr.2005.0384